Strain and surface phenomena in SiGe structures

A. Fischer, H. Kühne, M. Eichler, F. Holländer, and H. Richter
Institute for Semiconductor Physics, Walter-Korsing-Straβe 2, D-15230 Frankfurt (Oder), Germany
(Received 6 May 1996)

We present an approach in equilibrium theory for strain relaxation in heteroepitaxial semiconductor structures, which includes surface relaxation effects and elastic interactions between straight misfit dislocations. The free-surface boundary conditions are satisfied by placing an image dislocation outside the crystal so that its stress field cancels that of the real interface misfit dislocation at the surface. The effect of the Airy stress function that removes the fictitious shear and normal stresses at the surface is discussed. This image method provides an equilibrium theory, which correctly predicts experimentally observed values of critical strained layer thickness and completely describes the elastic and plastic strain relief and work hardening in lattice-mismatched SiGe epilayers. It is shown that the elastic coherency stress of the strained material is really affected by a large surface relaxation stress. This is essential for experimental determination of the Ge content of extremely thin films as a function of the tetragonal distortion of the cubic lattice cells. The equilibrium theory is also used to define the degree of strain relaxation and to predict the incomplete strain relief at the end of thermal relaxation process of metastable SiGe/Si heterostructures. [S0163-1829(96)02936-0]

I. INTRODUCTION

In the past few years the epitaxial growth of lattice-mismatched layers has attracted interest. The growth of coherent thin layers on rigid crystalline substrates is possible when biaxial compressive or tensile strain in the layer accommodates the lattice mismatch between the film and substrate material. When the stored strain energy exceeds a certain threshold, the heterostructure becomes metastable and the film strain may give way to misfit dislocations. The basic energetic and kinetic parameters describing mismatch accommodation by elastic strain and misfit dislocation in metastable heterostructures appear to be well described by the framework of Matthews and Blakeslee[1] and Dodson and Tsao.[2] However, it is evident that they cannot adequately explain the point of strain relief onset via plastic flow and the work hardening behavior of strained layers at the end of thermal relaxation process. This stems from ignoring the effects of elastic surface relaxation on the film lattice cells and the elastic interaction between straight misfit dislocations within the film-substrate interface. The first includes the problem of developing a relationship between the equilibrium critical thickness at which dislocations form and the bulk lattice mismatch. The latter involves balancing the force required to move misfit dislocations against the internal elastic stress field due to dislocation-dislocation interactions.[3] Finally, suffice it to say that classical equilibrium and kinetic models for strained layer case do not imply rigorously the conditions of equilibrium at the boundary.

In this paper we present a modified Volterra approach in equilibrium theory for strain relaxation in metastable heteroepitaxial semiconductor structures, which includes the surface effects on mismatch accommodation by tetragonal distortion of the cubic lattice cells and the elastic interaction between straight misfit dislocations. Because of the mathematical complexities involved in a proper atomistic description of the competing forces, the subject is not treated here in a Frenkel-Kontorowa model or its approximations. The principle of our theoretical method is straightforward. The free-surface boundary conditions are satisfied by placing an image dislocation outside the crystal so that its stress field cancels that of the real misfit dislocation at the surface. We will discuss the effect of the Airy stress function that removes the fictitious shear and normal stresses at the crystal surface and thus makes the crystal stress-free. We show that this image method provides an equilibrium theory that correctly predicts experimentally observed values of critical layer thickness. To demonstrate the physical significance of the present approach in equilibrium theory for strained layer relaxation, we have calculated the equilibrium critical thickness and Ge content via coherency strain of SiGe/Si strained layer structures and compared our results to those predicted by using relaxation models based on the absence of surface relaxation effects and elastically noninteracting dislocations. Furthermore, by considering the exact solution for the elastic interaction of real and image dislocations, our equilibrium model can completely describe the strain relief via lattice distortion, plastic flow, and work hardening in lattice mismatched epilayers. We show that our Volterra dislocation model is also appropriate when the film thickness is smaller than the misfit dislocation spacing and approaches dislocation core dimensions. It is pointed out that the elastic coherency stress of the strained material is really affected by a large surface relaxation stress. This is essential for experimental determination of the Ge content of extremely thin films as a function of the tetragonal distortion of the cubic lattice cells. The equilibrium theory is also used to define the degree of strain relaxation and to predict the incomplete strain relief at the end of thermal relaxation process of metastable SiGe/Si heterostructures. We consider here only the thermodynamic equilibrium and homogeneous deformations of strained layer structures, recognizing that kinematic factors can influence the attainment of the equilibrium state of strain.

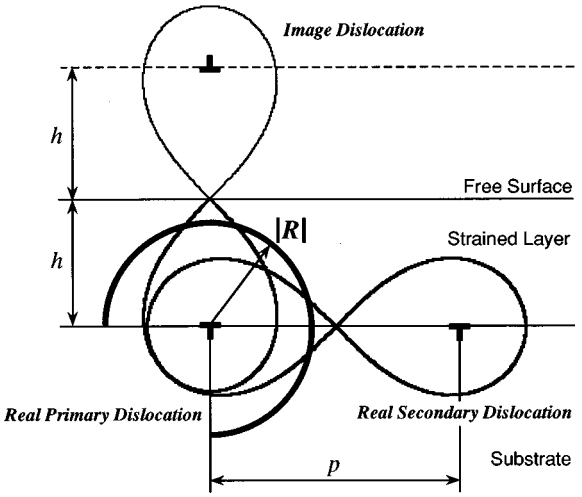

FIG. 1. Schematic illustration of the configuration of real and image misfit dislocations in a strained heteroepitaxial structure. The modulus of complex dislocation semispacing $|\mathbf{R}|$ is indicated.

II. FORCE BALANCE MODEL FOR STRAINED LAYER RELAXATION

In thermodynamic equilibrium, misfit dislocations appear at the interface of a strained layer heterostructure when the strained layer is thick enough that it is energetically favorable for the mismatch to be accommodated by a combination of elastic strain and interfacial misfit dislocations rather than by elastic strain alone.[4] This equilibrium critical thickness h_{crit} has been calculated and discussed by many authors[1,2,5–7] in the continuum picture as well as through phenomenological description of dislocation dynamics. However, there have been many reports, e.g., in Refs. 7 and 8, of experimental determinations of h_{crit} indicating that coherence apparently persists to thicknesses much greater than that predicted by classical equilibrium theories. The semiempirical kinetic model of Dodson and Tsao[2] is more appropriate to describe the latter stages of relaxation, where the effective stress is decreasing due to a reduction in misfit strain produced by the high dislocation density. For the case of sufficiently low dislocation content in the strained layer near the point of strain relief onset, this model reduces to the equilibrium form of Matthews and Blakeslee.[1] Thus the challenge remains to develop a predictive model appropriate for strained layer relaxation.

To introduce an appropriate continuum model, we begin by analyzing the conditions under which the strained layer relaxation should occur in metastable heterostructures then modify the governing models to account for the discrepancies mentioned above. In a finite body, boundary conditions at the surface must be satisfied. For example, no forces can act on a free surface. The image-force method provides a powerful tool to solve such problems in the continuum theory of elasticity.[9] Let us now consider the schematic illustration in Fig. 1. For the strained layer case, the free-surface boundary conditions are satisfied by placing an image dislocation outside the crystal such that its stress field cancels that of the real interfacial misfit dislocation at the surface. The condition is fulfilled if the self-stress of an image misfit dislocation of equal strength and opposite sign at a position $2h$ along the strained interface normal is superposed on the self-stress of the real primary dislocation. In general, the complete stress distribution for a mixed dislocation is given by the superposition of the stress fields of the real dislocation, the image dislocation, and a stress term derived from the Airy stress function that makes the surface traction-free. In our case of a mixed dislocation in a co-axial cylinder with its line parallel to the surface, the image construction gives the dominant part of the shear stress component. Since the corresponding stress function term exerts no force component along the strained interface normal, the shear stress of the dislocation construction is approximately obtained from the shear stress of the image dislocation alone. Notice that only shear stresses in the slip system produce glide forces on a dislocation.

In the continuum picture, the presence of dislocations causes strains around the line and, as a response to these, stresses as known from conventional elasticity theory. These stresses are defined by the contact forces transmitted through internal area elements. We speak of self-stresses to distinguish them from the applied misfit stresses. In linear approximation, the Volterra expression for the shear self-stress σ_s of a mixed straight dislocation due to its line tension in a region bounded by a coaxial cylinder of radius R is

$$\sigma_s=\frac{Gb(1-\nu\cos^2\theta)}{4\pi(1-\nu)R\cos\phi}\left(\ln\frac{\alpha R}{b}-1\right), \tag{1}$$

where G is the anisotropic shear modulus in the $\langle 110\rangle$ direction of the (001) plane of the epilayer material, ν is its Poisson ratio, b is the magnitude of the Burgers vector, θ is the angle between the dislocation Burgers vector and its line direction, ϕ is the angle between the slip plane and the strained interface normal, and α is a factor that accounts for the energy in the dislocation core where linear elasticity does not apply. α is generally taken to be in the range from 1 to 4 for covalently bonded semiconductor materials.[9] Because of the logarithmic dependence and the $R\gg b$ Volterra regime, the elastic self-stress is insensitive to the precise value of α. We set $\alpha/2.7=1$. Here σ_s is considered to act on the plane containing the dislocation line direction and the interface normal. So, referred to the slip plane surface, the shear component of the self-stress of a straight dislocation τ_s is given by $\tau_s=\cos\phi\,\sigma_s$. For our case, an interfacial 60°-type misfit dislocation on the slip plane causes resolved shear stress, i.e.,

$$\tau_s=\frac{Gb\left(1-\frac{\nu}{4}\right)}{4\pi(1-\nu)R\cos\phi}\ln\frac{R}{b}. \tag{2}$$

The ratio $G/\cos\phi$ is the isotropic shear modulus in the $\{111\}$ slip planes. Thus, in this case the quantity $b\tau_s$ is an image force given by the simple image construction. Under these conditions the attraction of the real primary dislocation toward the surface is obtained from the stress of the image dislocation alone.

So far we have considered the image-force and shear self-stress problems for a misfit dislocation in a metastable heterostructure. As shown in Fig. 1, imagine now a real secondary dislocation of equal strength and sign lying parallel to the real primary dislocation at a distance of p and moving continuously towards the primary dislocation. For further defor-

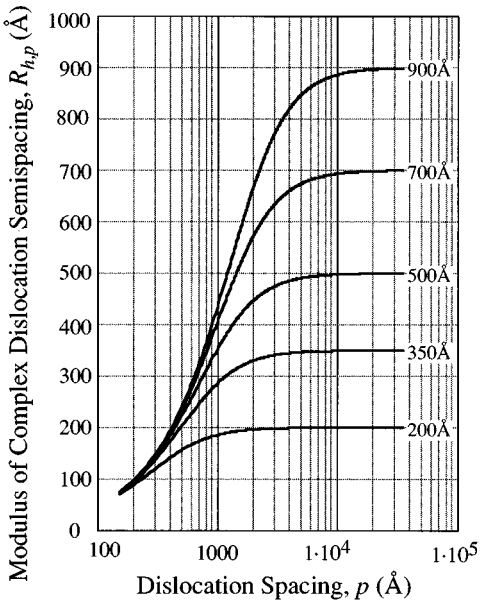

FIG. 2. Plot of the calculated modulus of complex dislocation semispacing $|\mathbf{R}|=R_{h,p}$ as a function of misfit dislocation spacing p for different strained layer thicknesses h.

mation under the driving force produced by the external misfit stress, it is necessary that the moving misfit dislocation overcomes the resistance caused by superposed shear self-stress field of the image dislocation and the real primary dislocation bounded by a virtual cylinder of radius $R=h$. Note that at larger distances from the real primary dislocation the image stresses largely cancel the dislocation stresses. Now for the elastic shear stress field extension of the real interfacial misfit dislocations lying parallel to another, a reasonable approximation would be to take roughly one-half the distance p between dislocations for R in Eq. (2).[9] However, in this case the quantity $b\tau_s$ is a real repulsive force that drives the real primary dislocation in its slip plane toward the surface. According to the Green function method for the elastic displacements $u(R)\propto b/R^2$ and the principle of superposition of displacement fields,[9] we now combine the imaginary, i.e., fictitious, and the real free-surface term of the shear self-stress of a misfit dislocation, i.e., h and $p/2$, respectively, and get a complex dislocation semispacing $\mathbf{R}$ as the first-order solution. Its modulus $|\mathbf{R}|=R_{h,p}$ is given by

$$\frac{1}{R_{h,p}^2}=\frac{1}{h^2}+\frac{4}{p^2}, \tag{3}$$

where h is the thickness of the epilayer and the subscripts h and p stand for the fictitious and the real component, respectively. We can say that the modulus of complex dislocation semi-spacing $R_{h,p}$ is an approximate solution for the stress-free boundary associated with the presence of two free surfaces. The relationship represented by Eq. (3) is plotted in Fig. 2 for different layer thicknesses h. The pursual of Fig. 2 shows some interesting relationships. For dislocation spacings p greater than $5h$, the modulus of complex dislocation semispacing as a measure of the extension of the elastically strained continuum about a misfit dislocation is dominated by its fictitious term, i.e., by the layer thickness h. In this case, Eq. (3) reduces to $R_{h,p}\sim h$. If p diminishes continuously, then the effect of the real term on $R_{h,p}$ increases slowly. When the dislocation spacing reaches the value $p\sim 2h$, the fictitious and the real free-surface terms make the same contribution to the modulus of complex dislocation semi-spacing. Below $p\sim h/5$, as the real misfit dislocations approach one another, the effect of the fictitious component vanishes and $R_{h,p}$ does not depend on h. Replacing R with $R_{h,p}$ in Eq. (2), the shear component of the total self-stress created by present dislocation content in a finite body becomes finally

$$\tau_s=\frac{Gb\left(1-\frac{\nu}{4}\right)}{4\pi(1-\nu)R_{h,p}\cos\phi}\ln\frac{R_{h,p}}{b}. \tag{4}$$

We notice that, up until now, we have considered a type of plane strain deformation under shear stresses, in which the body undergoes only changes of shape, but no changes of volume. Now let us consider the effect of the Airy stress function, which removes the fictitious tangential and radial normal stresses at the cylinder surface and thus changes the volume of the epilayer.

III. SURFACE RELAXATION STRESS

In the case of the normal self-stress components of 60° misfit dislocations the above solution is inadequate and large additional stresses must be superposed. For such dislocations the normal self-stress components given by the simple image construction do not vanish at the free surface. The procedure for solving this case is the same as that outlined above: first to superpose the simple image and then to devise a stress function that cancels the remaining forces acting at the free surface and thus satisfy the boundary conditions. Hirth and Lothe[9] have given the explicit solution of the Airy stress function for a pure edge dislocation in a cylinder parallel to a free surface. In analogy to the edge dislocation case, the first-order solution for a straight 60° misfit dislocation gives the normal self-stress components $\sigma_{f,t}$ and $\sigma_{f,r}$ that remove the fictitious plane strain and make the crystal stress-free:

$$\sigma_{f,t}=\frac{Gb\left(1-\frac{\nu}{4}\right)}{2\pi(1-\nu)\cos\phi}\left(\frac{3\eta}{h^2}-\frac{b^2}{\eta^3}\right), \tag{5a}$$

$$\sigma_{f,r}=\frac{Gb\left(1-\frac{\nu}{4}\right)}{2\pi(1-\nu)\cos\phi}\left(\frac{\eta}{h^2}+\frac{b^2}{\eta^3}\right), \tag{5b}$$

where η is the distance from the interface to the crystal surface. These tangential and radial stress terms are in fact the external state of stress that gives rise to the image dislocation construction that in turn creates the state of tension within the epilayer. Then, according to the generalized Hooke law, the normal stress $\sigma_{f,n}$ acting perpendicular to the slip plane is given by the combined effect of the tangential $\sigma_{f,t}$ and radial $\sigma_{f,r}$ stress components on the slip plane. Therefore, from Eqs. (5a) and (5b) we can write the relation

$$\sigma_{f,n}=\frac{1+2\nu}{(1-2\nu)(1+\nu)}\,2G(1+\nu)\,\frac{b\left(1-\frac{\nu}{4}\right)}{2\pi(1-\nu)\cos\phi}\,\frac{\eta}{h^2}. \tag{6}$$

Here $2G(1+\nu)$ is the Young modulus of the epilayer. $\sigma_{f,n}$ creates a state of tension between the slip planes of the epilayer. We call the normal stress $\sigma_{f,n}$ the ''surface relaxation stress.'' A transformation of this normal stress into the interface plane with the tensile axis normal to the dislocation line gives the state of in-plane tension within the epilayer. In these coordinates, Eq. (6) yields the in-plane surface relaxation stress σ_f. We get $\sigma_f=2\cos\lambda\,\sigma_{f,n}\cos\phi/\cos^2\phi$, where λ is the angle between the Burgers vector and the direction in the interface, normal to the dislocation line. For typical values of ν from 0.26 to 0.28, the quantity $(1+2\nu)(1-\nu/4)/\pi(1-2\nu)(1+\nu)\cos^2\phi$ varies from 1.1 to 1.2, close to unity. Thus the result for the in-plane surface relaxation stress becomes approximately

$$\sigma_f=\frac{2G(1+\nu)}{1-\nu}\,b\,\cos\lambda\,\frac{\eta}{h^2}. \tag{7}$$

In words, the in-plane surface relaxation stress decreases linearly from its maximum value at the crystal surface $\eta=h$ to zero at the interface $\eta=0$, whereas the strength of surface relaxation effects on the strained layer structure is related to the reciprocal of the square of the layer thickness h. Obviously, it is a remarkable result with regard to our considerations of the lattice-mismatch accommodation. When these effects are ignored and a coherency strain calculation is carried out, one obtains a spurious result leading to an erroneous misfit strain or Ge content of the SiGe layer. In addition, these effects should play a role in the lattice resistance to plastic flow of the material. For practical purposes, a reasonable approximation would be to take an average value σ_f^{av} for $\sigma_f(\eta)$, i.e.,

$$\sigma_f^{\mathrm{av}}=\frac{1}{h}\int_0^h\sigma_f(\eta)\,d\eta=\frac{2G(1+\nu)}{1-\nu}\,\frac{b\,\cos\lambda}{2h}. \tag{8}$$

Notice once again that G is the anisotropic shear modulus in the $\langle 110\rangle$ direction of the (001) plane of the epilayer. Furthermore, we have measured the effect of the elastic surface relaxation on the strained layer heterostructure directly. The results are presented in Sec. V.

IV. INTERACTION BETWEEN INTERNAL STRESS AND EXTERNAL STRESS

For a complete description of the equilibrium state of stress in lattice mismatched epilayers, we should now consider the resolved shear stress τ that acts on the slip system as a consequence of an externally applied misfit stress. In an initially misfit dislocation-free substrate-epilayer system, the in-plane strain ε is given by $(a_l-a_s)/a_s$, where a denotes the bulk lattice parameter and the subscripts s and l refer to the substrate and the layer, respectively. When the elastic strain is partially relieved by a single array of misfit dislocations created at the interface, the residual in-plane strain becomes $\varepsilon=[(a_l-a_s)/a_s]-(b\,\cos\lambda/p)$, where the term $b\,\cos\lambda/p$ represents the strain relief via plastic flow.[10] Here p is the average distance between the dislocations. Hence it follows that the lattice-mismatch accommodation would occur without in-plane tension within the epilayer caused by the surface relaxation stress. In other words, as explained above, for the case where $p>h/5$, the heterostructure is not traction-free, because normal stress components acting on the crystal surface are not taken into account. To overcome this difficulty we will now substitute the modulus of complex dislocation semispacing $R_{h,p}$ for $p/2$ in the residual in-plane strain expression above. So the true residual in-plane strain becomes $\varepsilon=[(a_l-a_s)/a_s]-[b\,\cos\lambda/(2R_{h,p})]$, where the h term accounts for the purely elastic surface relaxation and the p term for plastic flow. In this case, the resolved shear stress τ acting on the slip system on a misfit dislocation is given by

$$\tau=\cos\lambda\,\cos\phi\,\frac{2G(1+\nu)}{(1-\nu)\cos\phi}\left(\frac{a_l-a_s}{a_s}-\frac{b\,\cos\lambda}{2R_{h,p}}\right). \tag{9}$$

Thus the surface relaxation stress term is implied in the expression for the resolved shear stress that produced the driving force for plastic flow of the crystal. Note that the ratio $G/\cos\phi$ is the isotropic shear modulus in the {111} slip planes.

As we have previously argued, a finite heterostructure is subjected to point and lattice mismatch forces. The stresses and strains caused by such internal and external sources of stress can be superposed. We should now consider the resolved shear stress that acts on the slip system as a consequence of the externally applied misfit stress and the elastic shear stress field due to dislocation-dislocation interactions. As shown above, during misfit strain relief via plastic flow, an intrinsic elastic stress field is built up. For further deformation, the moving misfit dislocations have to overcome the resistance caused by this stress field. Consequently, the dislocation shear self-stress field is in the direction opposite the applied misfit stress. The excess resolved shear stress required to produce plastic flow will then be given by the difference between the two stress components. Equations (4) and (9) yield $\tau_{\mathrm{exc}}=\tau-\tau_s$, where the second term also accounts for work hardening of the material. Combining the two terms, we obtain an expression for the excess resolved shear stress:

$$\tau_{\mathrm{exc}}=\cos\lambda\,\cos\phi\,\frac{2G(1+\nu)}{(1-\nu)\cos\phi}\left[\frac{a_l-a_s}{a_s}-\frac{b\,\cos\lambda}{2R_{h,p}}(1+\beta)\right], \tag{10}$$

with

$$\beta=\frac{1-\frac{\nu}{4}}{4\pi\,\cos^2\lambda\,\cos\phi(1+\nu)}\ln\frac{R_{h,p}}{b}.$$

Here the quantity $[b\,\cos\lambda/(2R_{h,p})]\beta$ corresponds to the decrease in active shear stress through elastic interaction between dislocations depending on the current misfit dislocation density of the crystal.

As a final topic, a few words on the expression for the excess resolved shear stress are appropriate. This is a conve-

nient expression. The applications are numerous: problems of elastic strain retained by the epilayer, equilibrium critical thickness of a SiGe layer on Si substrate, initial and residual in-plane strain, film stress, work hardening of the material, degree of elastic and plastic strain relaxation, and misfit dislocation density reached at the equilibrium strain state, for example. Some of the applications are discussed in the following sections.

V. CRITICAL THICKNESS AND FILM STRESS OF SiGe/Si LAYERS

To demonstrate the physical significance of the present approach in equilibrium theory for strained layer relaxation proposed here, we have calculated the equilibrium critical thickness of $Si_{1-x}Ge_x$/Si strained layer structures as a function of the fractional atomic Ge content x. We have compared our results with those predicted by classical relaxation models, which do not include surface relaxation effects and dislocation-dislocation interactions. Taking the in-plane misfit strain $\varepsilon = 0.0418x$, Eqs. (3) and (10) and the equilibrium conditions for the point of strain relief onset via plastic flow, i.e., $\tau_{exc}=0$ and $p\rightarrow\infty$, lead to the following expression for the critical strained layer thickness h_{crit}:

$$x = \frac{b\ \cos\lambda}{0.0836 h_{crit}}\left[1 + \frac{1-\frac{\nu}{4}}{4\pi\ \cos^2\lambda\ \cos\phi(1+\nu)}\ln\frac{h_{crit}}{b}\right]. \tag{11}$$

In the absence of surface relaxation forces, the equilibrium critical thickness of a single strained epilayer upon a substrate of different lattice parameter according to Matthews and Blakeslee is given by the formulation reported in Ref. 1. Inserting appropriate material parameters in Eq. (11) and in the Matthews-Blakeslee formulation, $\cos\lambda = 0.5$, $\cos\phi = 0.816$, $\nu = 0.278$, and $b = 3.84$ Å for growth on the (001) surface, the equilibrium critical thickness calculated for the two different models are plotted in Fig. 3. It is seen, at first glance, that our values of h_{crit} represented by Eq. (11) are much larger than the values calculated using equation of Matthews and Blakeslee. Moreover, for a fractional atomic Ge content x greater than 0.5, the Matthews-Blakeslee formulation does not provide any value for h_{crit}. Additionally, we have compared our theoretical results with the published experimental data[7,8] of h_{crit} obtained from $Si_{1-x}Ge_x$/Si structures, grown by molecular-beam epitaxy at a growth temperature of 750 °C. For each composition, there is good agreement between our theoretical results and experimental data reported in Refs. 7 and 8. For example, for $x = 0.25$, h_{crit} was found to be approximately 200 Å. As seen in Fig. 3, for this case, our analysis yields the value of 200 Å. The Matthews-Blakeslee model predicts only an equilibrium critical thickness value of 60 Å.

So far, we have been considering the equilibrium critical thickness of a coherently strained structure. Let us now consider film stresses for elastically strained $Si_{1-x}Ge_x$/Si layers. For the pseudomorphically strained layer case, where $p\rightarrow\infty$, according to the previous Eq. (9), the in-plane film stress σ becomes

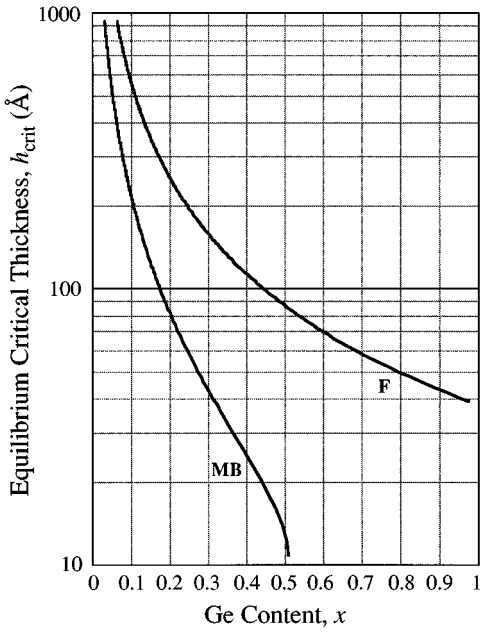

FIG. 3. Comparison of predicted equilibrium critical thickness h_{crit} for relaxation models based on a non-stress-free body (MB, Matthews-Blakeslee) and a stress-free body (F, this study) as a function of Ge content x.

$$\sigma = \frac{2G(1+\nu)}{1-\nu}\left(0.0418x - \frac{b\ \cos\lambda}{2h}\right). \tag{12}$$

This equation can then be used to predict the stress response to a strain increment, which is related to the volume change of the layer. The first term on the right-hand side corresponds to a volume expansion due to Ge incorporation and the second one to a volume contraction via surface relaxation. Thus the residual in-plane strain is given by $\varepsilon = 0.0418x - (b\ \cos\lambda/2h)$. For thin layers, this relation is essential for experimental determination of x as a function of the tetragonal distortion of the cubic lattice cells. Figure 4 shows a

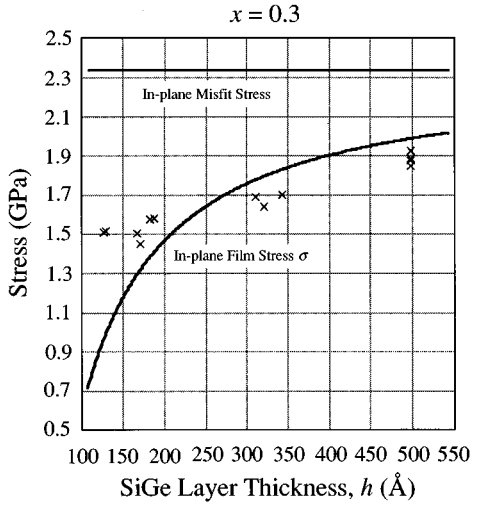

FIG. 4. Theoretical (solid line) and experimental (×) in-plane epitaxial film stress σ as a function of thickness h for as-grown SiGe/Si. The in-plane misfit stress (elastic coherency stress) corresponding to a strain of $0.0418x$ is also shown.

plot of σ versus h for $x=0.3$ and $G=51$ GPa. This relation between coherency stress and surface relaxation stress has been studied experimentally too. The in-plane epitaxial film stress σ as a function of layer thickness was measured by a thin-film stress measuring apparatus, which measures the changes in the radius of curvature of a substrate created by deposition of a stressed thin film on its surface. Our experimental data are also shown in Fig. 4. To our knowledge, such measurements of surface relaxation stresses have not been reported previously. It is seen that there is good agreement between our theoretical results and experimental data. This tells us that the elastic coherency stress of the strained material in the plane of the surface is really affected by a large surface relaxation stress. Consequently, as stated previously, calculations of the Ge composition x for SiGe epitaxy based only on misfit strain values assuming bulk lattice spacings could be seriously in error.

VI. PLASTIC DEFORMATION AND WORK HARDENING IN SiGe/Si

SiGe/Si structures may be grown to substantially greater thickness than our equilibrium critical thickness predictions, before misfit dislocation nucleation and propagation are observed. The heterostructure becomes metastable during growth because $\tau_{\text{exc}}>0$. This metastable growth regime is concerned with the initial period of creep of diamond structure materials, in which marked plastic deformation under static load does not start abruptly. In our case of strained layer relaxation, such an initial period is characterized by an incubation time encouraged by lower growth temperature and lattice mismatch. The initial creep period is finally terminated by the onset of in-plane strain relief via plastic flow.

The ramifications of our model for plastic flow and work hardening in $Si_{1-x}Ge_x$/Si strained layer structures will now be discussed. According to Eq. (9), the in-plane film stress σ becomes

$$\sigma=\frac{2G(1+\nu)}{1-\nu}\left(0.0418x-\frac{b\ \cos\lambda}{2R_{h,p}}\right). \tag{13}$$

Putting the values of the material parameters into Eqs. (10) and (13), $\cos\lambda=0.5$, $\cos\phi=0.816$, $G=51$ GPa, $\nu=0.278$, and $b=3.84$ Å, assuming a metastable epilayer with $x=0.3$ and $h=500$ Å, and recalling Eq. (3), we can evaluate the variation in excess resolved shear stress acting on the slip system τ_{exc} and in-plane epitaxial film stress σ for the complete thermal relaxation process. At the beginning of deformation, where $p\to\infty$, $\tau_{\text{exc}}=0.7$ GPa, and $\sigma=1.9$ GPa, as illustrated in Fig. 5. During plastic flow via misfit dislocation generation and propagation, τ_{exc} and σ diminish continuously and then remain unchanged at zero and 1.15 GPa, respectively, whereas the shear self-stress component τ_s rises to its maximum value. At this equilibrium deformation stage, the externally applied misfit stress and the shear component of elastic stress field due to dislocation interaction compensate one another and strain relief via plastic flow comes to rest. Thus, as a result of work hardening, the lattice mismatched epilayer will remain in a certain state of strain at the end of thermal relaxation process, i.e., the strained layer is in a stable state.

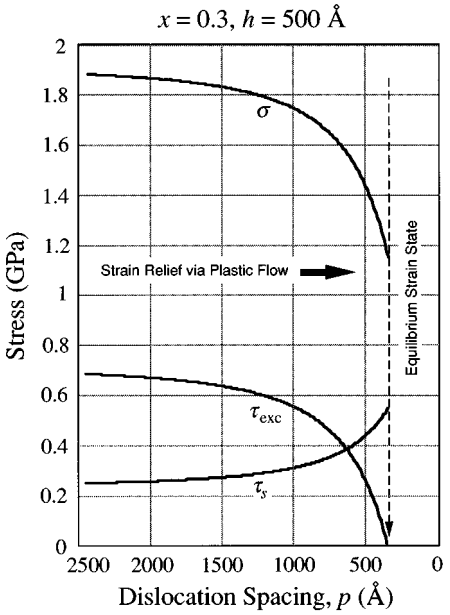

FIG. 5. Decrease in the in-plane epitaxial film stress σ and excess resolved shear stress τ_{exc} during strain relief via plastic flow as a function of the dislocation spacing p. The direction of strain relief via plastic flow and the equilibrium strain state at the end of the thermal relaxation process are indicated.

It should be mentioned here that recent investigations by Gillard, Nix, and Freund[11] suggest that dislocation blocking plays a certain role in limiting strain relaxation. We believe, as shown in the present and the previous sections, that the creep process in all the stages of strain relaxation in these structures is essentially determined by a purely elastic interaction between dislocations, which leads ultimately to work hardening of the material. Further experiments would be required to assess the relative contribution from blocking mechanism.

For homogenous deformation, our equilibrium theory for strained layer relaxation is able to predict the degree of in-plane misfit strain relaxation both at the point of onset of plastic flow and at the point of equilibrium strain state where the plastic flow comes to rest. Returning to Eq. (13), which is the general in-plane film stress equation, we define the degree of strain relaxation γ as the relative lattice-mismatch accommodation by elastic surface relaxation and interfacial misfit dislocations compared to mismatch accommodation by the elastic in-plane strain alone. It can be written as the ratio of the in-plane strain relief to the in-plane strain (coherency strain). For $Si_{1-x}Ge_x$/Si heterostructures, we get

$$\gamma=\frac{b\ \cos\lambda}{0.0836xR_{h,p}}. \tag{14}$$

For the point of strain relief onset via plastic flow, where $p\to\infty$, Eq. (14) reduces to $\gamma_{\text{el}}=b\ \cos\lambda/0.0836xh$, which can be a general expression for the degree of elastic strain relief via surface relaxation. γ_{el} is a constant for a given metastable or stable SiGe/Si strained layer system. Again, according to Eq. (14), the degree of total strain relaxation $\gamma_{t(0)}$ for the point of equilibrium strain state at the end of thermal relaxation process is given by $\gamma_{t(0)}=b\ \cos\lambda/0.0836xR_{h,p(0)}$,

where the subscript $p(0)$ stands for the misfit dislocation spacing reached at the equilibrium deformation stage. In our case, for $Si_{0.7}Ge_{0.3}/Si$, $h=500$ Å, we get $\gamma_{el}=0.15$ and $\gamma_{t(0)}=0.49$ with $p(0)=330$ Å. As the corresponding degree of plastic strain relaxation is $\gamma_{pl(0)}=\gamma_{t(0)}-\gamma_{el}$, we thus have $\gamma_{pl(0)}=0.34$. Thus, as stated previously, the lattice-mismatched epilayer remains in a certain state of strain at the end of thermal relaxation process. For the given heterosystem, as a result of work hardening, the residual in-plane strain is approximately 51%. Again, an elastic strain of 15% is retained in the epilayer by surface relaxation effects and about 34% of the in-plane strain due to lattice mismatch is relieved via plastic flow. It should be noted that, up to now, neither equilibrium theory was able to predict the correct relaxed strain in heteroepitaxial films.

VII. MISFIT AND THREADING DISLOCATIONS

Incomplete strain relief at the end of thermal relaxation process, as explained above, was also confirmed by us experimentally. Because of its importance for our equilibrium theory, we should now consider the main results briefly. The decrease of the in-plane epitaxial film stress σ as a function of time is measured from *in situ* relaxation experiments in the temperature range 800 °C–900 °C by the thin-film stress measuring apparatus. Metastable $Si_{0.7}Ge_{0.3}/Si$ samples with a strained layer, approximately 500 Å thick, were grown by molecular-beam epitaxy at a growth temperature of 550 °C. During postgrowth high-temperature relaxation, the measured film stress value diminishes continuously from 1.9 GPa up to 1.15 GPa and then remains unchanged at this value, as predicted by Eq. (13).

A Lang topograph image and an optical micrograph of misfit dislocation network and misfit dislocation terminations built at the equilibrium strain state are shown in Fig. 6. For an accurate determination of average interface dislocation spacing in highly dislocated material from the areal distribution of misfit dislocation terminations to the free surface, i.e., from the distribution of threading dislocations, a relationship between dislocation separation, dislocation length, and number of dislocations has been deduced in the following way. Figure 7 schematically shows the interfacial misfit dislocation network and the threading dislocations connecting the misfit segments to the free surface. The average line length of the misfit dislocations Λ in any area of the interface is given by $\Lambda=2/(p_T n_T)$, where p_T is the measured average minimum interfacial spacing of misfit dislocation terminations (threading dislocations) and n_T is the measured areal density of misfit dislocation terminations. The factor of 2 is included, because in (001) epitaxy, strain is relieved by two orthogonal misfit dislocation sets. The dislocation spacing p measured in each of the $\langle 110\rangle$ directions is the inverse of the linear misfit dislocation density $N=n_T A^n/2$, where A is the interfacial area occupied with two orthogonal misfit dislocation sets of the sizes given by the square of the average misfit dislocation length Λ^2. In general, the area exponent n varies between 0.5 and 1. In our case, for arrays of parallel interfacial 60°-type misfit dislocations, the theory of dislocations predicts a value of $n=1$. The average interface dislocation spacing then becomes $p=2e/(n_T\Lambda^2)$, where e is an unit length. According to the misfit dislocation length expression given above, we obtain

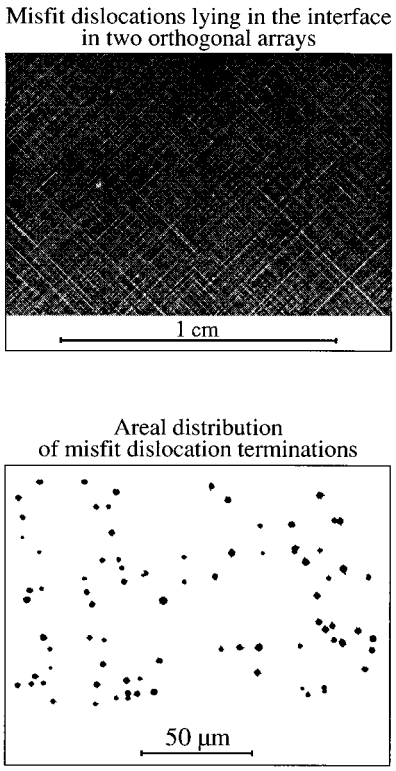

FIG. 6. Misfit dislocation network built at the end of the thermal relaxation process in 500-Å $Si_{0.7}Ge_{0.3}/Si$ heterostructures.

$$p=\frac{p_T^2 n_T}{2}\,e \tag{15}$$

and can thus determine p in terms of p_T and n_T, which we may measure from the areal distribution of misfit dislocation terminations.

Using Eq. (15), from the optical micrograph shown in Fig. 6, we have measured the misfit dislocation spacings reached at the end of the thermal relaxation processes. With $p_T\sim 4$

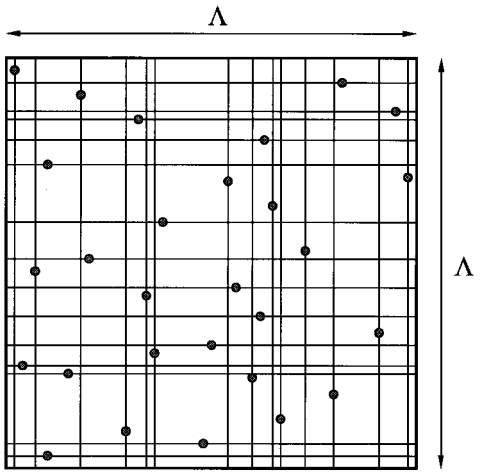

FIG. 7. Schematic illustration of the configuration of misfit dislocations and misfit dislocation terminations (threading dislocations). Lines represent misfit dislocation segments and dots are threading dislocations.

μm and $n_T \sim 0.004\ \mu m^{-2}$, the average misfit dislocation spacing p for the given strained layer system plastically deformed is observed to be approximately 300–350 Å. As seen in Sec. VI, this is consistent with our theoretical prediction of $p(0) = 330$ Å.

VIII. SUMMARY AND CONCLUSIONS

We have attempted to provide a physical basis for a different approach in equilibrium theory for strain relaxation in metastable heteroepitaxial semiconductor structures. This approach includes the surface relaxation effects on the strained layer structure and the elastic interaction between straight misfit dislocations. The main purpose of this work was to develop a straightforward treatment, valid in linear elasticity, for the relatively complicated case of deformation of a finite body containing internal stresses and subjected to lattice-mismatch forces. The model we have outlined yields an expression in terms of the excess resolved shear stress [Eq. (10)] for strained layer relaxation, so that the elastic strain retained by the epilayer, the equilibrium critical thickness of the strained layer, the initial and residual in-plane strain, the film stress, work hardening effects on the material, the degree of strain relaxation, and the misfit dislocation density, reached at the equilibrium strain state, can be predicted.

We believe that the image method proposed here provides an equilibrium theory that correctly predicts the coherency and relaxation behavior of SiGe/Si structures. Finally, this more refined model yields better agreement between computed and measured values and provides a consistent picture of the complex mechanism for strain relief and defect propagation in a strained layer on a lattice-mismatched substrate.

ACKNOWLEDGMENTS

The authors would like to thank Professor A. Ourmazd for helpful discussions and advice and are indebted to Dr. B. Tillack and Dr. H.-P. Zeindl for supplying CVD- and MBE-grown SiGe/Si material for this research.

[1] J. W. Matthews and A. E. Blakeslee, J. Cryst. Growth **27**, 118 (1974); **32**, 265 (1976).
[2] B. W. Dodson and J. Y. Tsao, Appl. Phys. Lett. **51**, 1325 (1987); **52**, 852 (1988).
[3] A. Fischer and H. Richter, Appl. Phys. Lett. **64**, 1218 (1994).
[4] G. C. Osbourn, IEEE J. Quantum Electron. **QE-22**, 1677 (1986).
[5] D. C. Houghton, Appl. Phys. Lett. **57**, 1434 (1990); **57**, 2124 (1990).
[6] R. Hull, J. C. Bean, D. J. Werder, and R. E. Leibenguth, Phys. Rev. B **40**, 1681 (1989).
[7] E. Kasper, in *Physics and Applications of Quantum Wells and Superlattices*, edited by E. E. Mendez and K. von Klitzing (Plenum, New York, 1987).
[8] R. People and J. C. Bean, Appl. Phys. Lett. **47**, 322 (1985).
[9] J. P. Hirth and J. Lothe, *Theory of Dislocations* (McGraw-Hill, New York, 1968).
[10] J. R. Willis, S. C. Jain, and R. Bullough, Appl. Phys. Lett. **59**, 920 (1991).
[11] V. T. Gillard, W. D. Nix, and L. B. Freund, J. Appl. Phys. **76**, 7280 (1994).